

A Regime-Switching Heston Model for VIX and S&P 500 Implied Volatilities

Andrew Papanicolaou* Ronnie Sircar†

October 2012, revised June 6, 2013

Abstract

Volatility products have become popular in the past 15 years as a hedge against market uncertainty. In particular, there is growing interest in options on the VIX volatility index. A number of recent empirical studies examine whether there is significantly greater risk premium in VIX option prices compared with S&P 500 option prices. We address this issue by proposing and analyzing a stochastic volatility model with regime switching. The basic Heston model cannot capture VIX implied volatilities, as has been documented. We show that the incorporation of sharp regime shifts can bridge this shortcoming. We take advantage of asymptotic and Fourier methods to make the extension tractable, and we present a fit to data, both in times of crisis and relative calm, which shows the effectiveness of the regime switching.

1 Introduction

Volatility derivatives have become popular at least since 1998, primarily through variance swaps. More recently, they have been viewed as indicators of the market's perception and quantification of future uncertainty. The VIX volatility index has become a household name as the "fear index". We present, analyze, and test to data a stochastic volatility model with regime switching that tries to capture the "spike-o-phobia" that seems apparent in the pronounced skew of the VIX options implied volatility surface.

Stochastic volatility jump-diffusion models are known to be effective in fitting the implied volatility of S&P 500 (SPX) options. However, VIX options cannot be fit by the widely-used Heston model because many of the strikes lie in the tail of the volatility process's distribution. Therefore, a model for consistent pricing of both VIX and SPX options should have a volatility process that has a distribution which spreads probability mass over a broader range than the standard square-root process. In this paper we propose the addition of a regime-switching process to the Heston model, a modeling feature that will widen the support of the bulk of the volatility process's probability distribution. The fits to data are qualitatively reasonable, but there is some disparity between the two markets, a finding also reported in recent econometric literature that we discuss below. The Heston model is an industry standard among stochastic volatility models. Its parameters are known to have clear and specific controls on the implied volatility skew/smile, and it can mimic the implied volatilities of around-the-money options with a fair

*ORFE Department, Princeton University, Sherrerd Hall, Princeton NJ 08544, apapanic@princeton.edu. Work partially supported by NSF grant DMS-0739195.

†ORFE Department, Princeton University, Sherrerd Hall, Princeton NJ 08544, sircar@princeton.edu. Work partially supported by NSF grant DMS-1211906.

degree of accuracy. A major shortcoming is that it is often unable to fit the implied skew of short-time-to-maturity options. Nevertheless, it is still widely used, and so it would be significant (both in practice and in theory) if it was shown that additional features such as jumps and regime-change allow it to effectively price VIX derivatives.

The formula for the price of a European call option in the Heston model was originally derived in [25], formulae for jump models are given in [28], and combined jump-diffusion models are analyzed in [2, 19]. In particular, a square-root process with jumps in both the underlying and the volatility was used in [32] to price VIX options. However, several studies have shown that VIX implied volatility data is not reproducible by models with volatility given by a square-root process [16, 23, 31]. Alternative models such as the 3/2-model have emerged as possible candidates for fitting VIX implied volatility [3, 15]. Another approach is to take VIX options or variance swap data directly into the model of the underlying S&P 500 index (SPX) so that it is consistent by design, but at the cost of the index dynamics depending on the maturity dates of the volatility derivatives. This is the market model approach taken in [13]. In [30], a simultaneous fit to VIX and SPX option prices is presented using Sato processes. Recently, [4] presents joint fits using a double mean-reverting diffusion model using Monte Carlo simulation.

However, there are several empirical papers that focus on the quality of the fits achieved. For instance [14] demonstrates the difficulty of fitting out-of-the-money VIX options well, while [12] finds that “the information content implied from these two option markets is not identical”. In a current working paper, [33] use nonparametric estimates of state price densities implied from SPX and VIX option markets and find that “VIX options deliver unique information for investors to extract information on volatility dynamics”. In many ways, the issues are how one interprets consistency and quality of fits, particularly if one demands good fits across all strikes and even short maturities, and the mixed message reflects more the practitioner or econometrics perspective of the authors.

In the time series literature, markets with Markov regime change were studied in [24], the importance of identifying regime change for GARCH models was identified in [26], and the importance of jumps was highlighted in [1, 5, 34, 31], where evidence from variance swap data suggests that fears regarding outlier events creates a premium that is most likely caused by jump risk. Elliott *et al.* [10, 11] propose an extended Heston model, where the parameters in the volatility process are modulated by a Markov chain, and they analyze the pricing of variance swaps and other derivatives. They demonstrate the impact of regime change by Monte Carlo experiments, but they did not consider VIX options valuation or calibration to data as we do here. In this paper, we specify a parametrically richer version of the Heston wherein the volatility process is modulated by a Markov chain that represents the regime state of the market’s volatility. The model also has a jump structure that depends on the regime change in such a way as to model the contrary motion between equity and volatility (i.e. the leverage effect). The rate of regime-change is taken to be of a small enough order so that option prices can be expanded with a power series. In this expansion, the lowest order term is the Heston model’s price and the first correction term can also be written as a function of the components of the Heston price. This is similar to the methodology in [20], except that they have added a fast-mean reverting diffusion to the Heston model whereas we have added a slow jump factor. In both their paper and ours, there are explicit formulae for the Fourier transform of the option price’s expansion.

When applied to data, we find that our model captures separately the implied volatility skews of both the SPX and VIX options (see Figures 6 and 7). But when the parameter estimates from VIX options are used to compute SPX option prices through the model, some systematic discrepancies between the two markets are revealed (see Figure 8), which highlights a distinction between the the VIX and SPX options markets. We also apply the model to VIX options from the 2008 financial crisis and to non-crisis data of 2011, and are able to relate the parameter estimates to the historical beliefs about volatility fears during

these periods

The rest of the paper is organized as follows: Section 2 provides an introductory analysis of the VIX and SPX time series data, along with some analysis of the implied volatility of VIX options; Section 3 describes the model that we're proposing, as well as the derivation of some key items such as the variance swap rate, the VIX formula, and a PIDE for option pricing; Section 4 derives an expansion for solving the pricing PIDE, for both the case of stock options and VIX options; Section 5 describes the procedure for calibrating the data to the pricing formulae (both for VIX and SPX options data) and also provides an empirical study of 2008 crisis data and some post-crisis data; Section 6 concludes.

2 Preliminary Data Analysis

To motivate our choice of model, we start by examining the market data. We'll look at time series data and the VIX options implied volatility skew; these empirical facts will give us some bearing on which features are important.

2.1 Time Series Analysis

Figure 1 shows the time-series plot of the SPX index and the VIX. It is well-known that a volatility

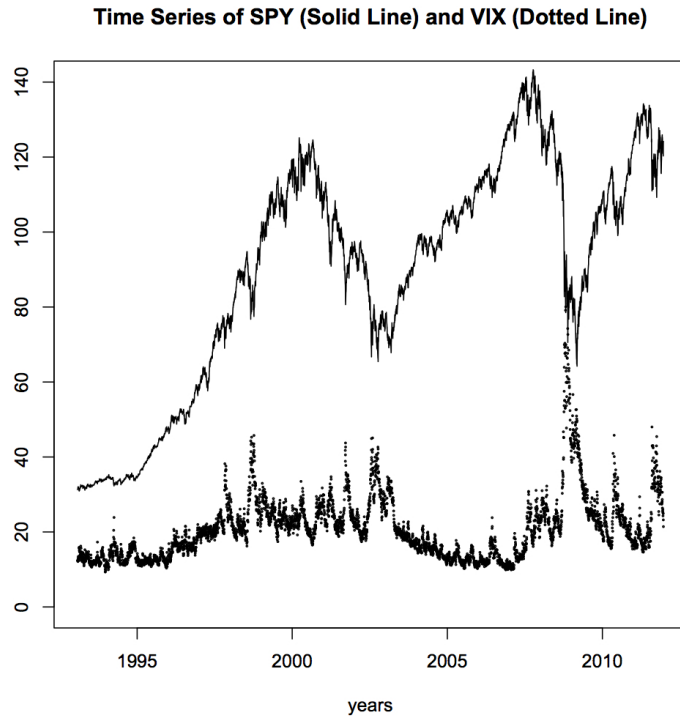


Figure 1: *The solid line is the time series plot of the SPX index, and the dotted line is the VIX index. The correlation of these time series is about -80%.*

leverage effect needs to be included in any useful model, and indeed, from the figure we can see an inverse relationship between the SPX and the VIX: bull markets are accompanied by low VIX, and bear markets

are accompanied by higher VIX. Empirically, the negative correlation between log-returns on SPX and log-returns on VIX is quite strong, usually around -60% to -80% . Furthermore, Figure 1 is interesting because it shows a time series over a period where the markets experience several macroeconomic shocks. There will be significantly higher correlation for time-windows with a couple of these shocks, compared to that of time windows where there are no shocks. Hence, negative correlation between S&P 500 and the VIX should be modeled with two components: correlated diffusion processes to account for the day-to-day microstructure fluctuations, and a jump process to model the singular events that shock the market. The importance of jumps for describing the volatility leverage effect is found in [34].

Heavy tails are another important feature that can be deduced from the time-series. Figure 2 shows the scatter plot of the log-returns on VIX against the log-returns on SPX, along with simulated returns sampled from various fits to bivariate distributions. It is clear from these scatter plots that simply fitting a

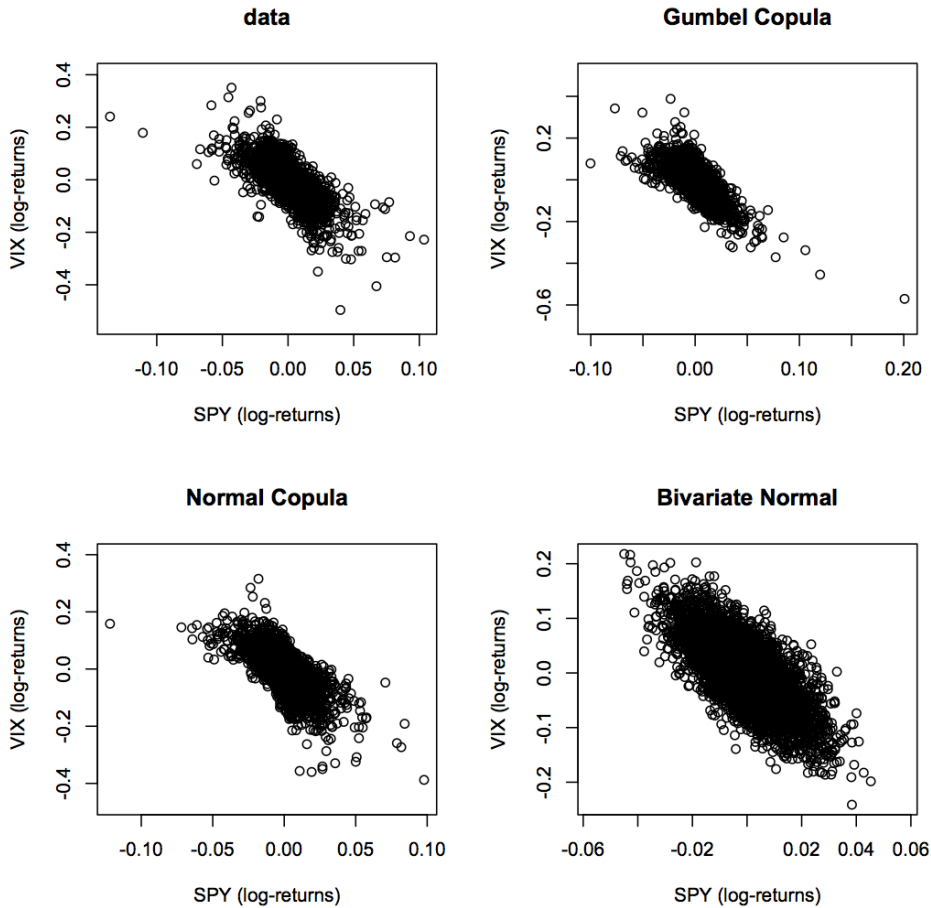


Figure 2: **Top Left:** The scatter plot of the log-returns on VIX against the log-returns on SPX. **Top Right:** Simulations from a fitted Gumbel copula. **Bottom Left:** Simulations from a fitted Gaussian copula. **Bottom Right:** Simulations from a fitted bivariate Gaussian distribution. Notice that the bivariate Gaussian simulation does not have enough outliers.

bivariate Gaussian distribution to log-returns is insufficient, and that the bivariate distribution of returns can be better-fitted with a copula. The copula fits in Figure 2 suggest that not only should there be

negative correlation between the log-returns of SPX and VIX, but there should also be jumps in both indices and these jumps should happen in opposite directions.

2.2 VIX Option Implied Volatility

For two times t and T with $t \leq T < \infty$, denote the future on VIX at time t with settlement date T as

$$F_{t,T} = \mathbb{E}_t \text{VIX}_T$$

where \mathbb{E}_t is the expectation under the market-chosen risk-neutral measure. The payoff on a VIX call option is $(F_{T,T} - K)^+$, and so the Black model for pricing an option on $F_{t,T}$ can be applied::

$$\begin{aligned} C^{BS}(F_{t,T}, T-t, r, K, \sigma) &= e^{-r(T-t)} (F_{t,T} \mathcal{N}(d_1) - K \mathcal{N}(d_2)) \\ d_1 &= \frac{\log(F_{t,T}/K) + \frac{\sigma^2}{2}(T-t)}{\sigma\sqrt{T-t}} \\ d_2 &= d_1 - \sigma\sqrt{T-t}, \end{aligned}$$

where $\mathcal{N}(\cdot)$ denotes the CDF of the standard normal distribution function. The implied volatility of this option is $\hat{\sigma}_t^{BS}(T, K)$ such that

$$C^{BS}(F_{t,T}, T-t, r, K, \hat{\sigma}_t^{BS}(T, K)) = C_t^{data}(K).$$

Implied volatilities for VIX options on April 8th, 2011 are shown in Figure 3. Some things are important to notice: there is a premium on low strike options as well as those with high strike; the low-point in the curve moves to the left of the future price as time-to-maturity increases; the overall level of volatility goes down as time-to-maturity increases. But most importantly, one should take note of the increase in implied volatility as strike increases. In [15, 16, 23, 31], it is recognized that this increase in implied volatility is a phenomenon which cannot be described by the Heston model, the reason being that the square-root process has relatively little probability mass outside the range of everyday values. Hence, outlier events being hedged by high-strike VIX options are under-priced by the Heston model. A useful model will have to account for this phenomenon.

3 Heston Model with Regime Change

We work on a probability space $(\Omega, \mathcal{F}, \mathbb{P})$ where \mathbb{P} is a risk-neutral or equivalent martingale measure. Let θ_t be a continuous-time Markov chain that represents the regime-state of volatility. The regime variable can take three values, $\theta_t \in \{1, 2, 3\}$ where $\{\theta_t = 1\}$ means that volatility is in its low state, $\{\theta_t = 2\}$ means it is in medium state, and $\{\theta_t = 3\}$ means it is in a high state. The probabilities of regime-change are given by the intensity matrix $Q \in \mathbb{R}^{3 \times 3}$, and the distribution of θ_t satisfies

$$\frac{d}{dt} \mathbb{P}(\theta_t = n) = \delta \sum_{m=1}^3 Q_{mn} \mathbb{P}(\theta_t = m) \quad \text{for } n = 1, 2, 3, \tag{1}$$

where $\delta > 0$ is a small parameter which creates a slow time scale in the regime. The log-price X of a stock (or index) and its volatility follow paths generated by the following stochastic differential equations

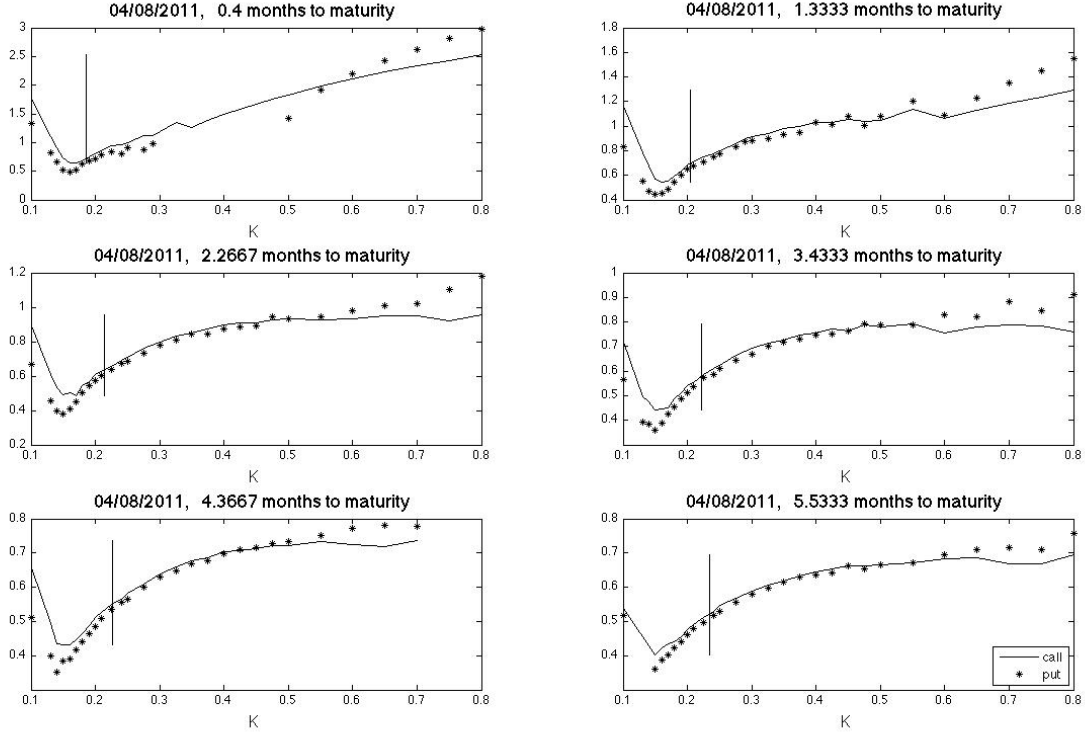


Figure 3: The implied volatilities of VIX call options (solid line) and put options (dotted line) on April 8th, 2011. The vertical black line is the future price with settlement data equivalent to the option expiry. Notice the higher implied volatility on low strike options as well as those with high strike; the low-point in the curve moves to the left of the future price as time-to-maturity increases; the overall level of volatility goes down as time-to-maturity increases.

(SDEs):

$$\begin{aligned} dX_t &= \left(r - \frac{1}{2} f^2(\theta_t) Y_t - \delta\nu(\theta_{t-}) \right) dt + f(\theta_t) \sqrt{Y_t} dW_t - \lambda(\theta_t) J_t dN_t , \\ dY_t &= \kappa(\bar{Y} - Y_t) dt + \gamma \sqrt{Y_t} dB_t , \\ dN_t &= \mathbb{1}_{[\theta_t \neq \theta_{t-}]} , \end{aligned} \quad (2)$$

where $r \geq 0$ is the risk-free rate of return, and W_t and B_t are Brownian motions with correlation $\rho \in (-1, 1)$ so that $\mathbb{E}\{dW_t dB_t\} = \rho dt$. The random jump sizes J_t are independent and identically distributed as exponential with parameter 1. Both J_t and the regime process θ_t are independent of the Brownian motions and of each other. The function λ controls the direction and magnitude of jumps in the stock price, and the function $\delta\nu$ compensates the jumps so that $e^{X_t - rt}$ is a martingale:

$$\delta\nu(n) = \lim_{\Delta t \searrow 0} \frac{\mathbb{E} \left[\int_t^{t+\Delta t} (e^{-\lambda(\theta_s) J_s} - 1) dN_s \mid \theta_{t-} = n \right]}{\Delta t} = - \sum_{m \neq n} \delta Q_{nm} \frac{\lambda(m)}{1 + \lambda(m)} ,$$

for $n = 1, 2, 3$, using the moment generating function $\mathbb{E}e^{-\lambda(m)J_s} = \frac{1}{1+\lambda(m)}$. Finally, parameters should be chosen to satisfy the Feller condition, $\gamma^2 \leq 2\kappa\bar{Y}$. This will ensure that Y_t stays strictly positive.

The Heston model is popular in pricing not only because it has an explicit (up to Fourier transform) formula, but because it has a handful of parameters that can be identified with effects that are observed in equity implied volatilities. Some motivation for and features of our model are:

- The persistence of high volatility levels when there is a jump in the stock price. Historically, precipitous drops in asset prices have been accompanied by spikes in volatility, and this is precisely what is accomplished by having an exponential random variable that is amplified by $\lambda(\theta_t)$: when volatility jumps to its high state there will be a drop in the stock price, and when volatility jumps to its low state there will be a short-lived surge.
- The parameter δ and the matrix Q quantify the intensity with which the market views the possibility of a change in the volatility state. Our assumption will be that δQ is of a relatively small order so that we can do an asymptotic series expansion of equity options; our pricing formula for VIX options will be exact.
- The regime process controls the level of volatility in the strategy of the VIX tail hedge (VXTH), which is one of the CBOE's indices for tracking the price of volatility risk. Volatility is considered to be in a low state when the VIX future is between 15% and 30%; a medium state when the VIX future is between 20% and 50%; and a high state when the VIX future is over 50%.¹

The model in (2) is fundamentally related to the jump models in [2] and [28], but the addition of the regimes and the additional structure in the jumps prevent us from pricing directly with an affine Fourier transform. Also, model (2) is a mixture model, as the future distribution of X_T and Y_T can be viewed as a mixture of three distributions, each of which is parameterized by a regime state.

3.1 Variance Swaps & the VIX

Volatility swaps, variance swaps and swaptions on realized variance are derivatives on X_t that have become liquid in OTC markets over the past few decades (see [6] for a general review of volatility derivatives). They provide the investor with an instrument that returns a positive cash flow in times of high volatility. European call and put options on VIX have also become liquid, but these options are considerably exotic as they are really an option on a basket of S&P 500 options (the VIX is itself a basket of S&P 500 options; see [7, 8] or chapter 11 of [22]), and so pricing a European option on VIX is somewhat like pricing a compound option on the stock.

Let \mathbb{E}_t denote the risk-neutral expectation given the filtration \mathcal{F}_t generated by $\{(X_s, Y_s, \theta_s) : s \leq t\}$. For $T > 0$, the **realized variance** of the stock up to time T is the quadratic variation of its logarithm:

$$[X]_T = \lim_{\|\mathcal{T}\| \searrow 0} \sum_{t_\ell \in \mathcal{T}} (X_{t_{\ell+1}} - X_{t_\ell})^2 \quad \text{where } \mathcal{T} \text{ is a partition of } [0, T] ,$$

which is referred to as the ‘floating-leg’ of a variance swap contract. For a variance swap contract occurring during the period $[t, t + \tau]$ for some $\tau > 0$, the swap rate (or the ‘fixed-leg’) is given by the expected

¹There is a VXTH white paper located at <http://www.cboe.com/micro/VXTH/documents/VXTHWhitePaper.pdf>.

quadratic variation of $\log(X_t)$ over the interval $[t, t + \tau]$. Then we have

$$\begin{aligned} \text{VS}_{t,\tau} &= \frac{1}{\tau} (\mathbb{E}_t[X]_{t+\tau} - [X]_t) \\ &= \frac{1}{\tau} \mathbb{E}_t \left(\int_t^{t+\tau} f^2(\theta_s) Y_s ds + \int_t^{t+\tau} \lambda^2(\theta_s) J_s^2 dN_s \right) \\ &= \frac{1}{\tau} \left(\int_t^{t+\tau} \mathbb{E}_t[f^2(\theta_s) Y_s] ds + 2\delta \sum_{n,m \neq n} [I(t; \tau)]_{\theta_t, n} \lambda^2(m) Q_{nm} \right), \end{aligned}$$

where we define the matrix I by

$$I(t; \tau) = \int_t^{t+\tau} \left[e^{\delta(s-t)Q} \right] ds.$$

Therefore,

$$\text{VS}_{t,\tau} = \frac{\bar{Y}}{\tau} \int_t^{t+\tau} \mathbb{E}_t[f^2(\theta_s)] ds + \frac{(Y_t - \bar{Y})}{\tau} \int_t^{t+\tau} e^{-\kappa(s-t)} \mathbb{E}_t[f^2(\theta_s)] ds + \frac{2\delta}{\tau} \sum_{n,m \neq n} [I(t; \tau)]_{\theta_t, n} \lambda^2(m) Q_{nm}. \quad (3)$$

In contrast to variance swap rates, the volatility swap rate is the expectation of the square-root of realized variance and is considerably more model-dependent and harder to compute. Formulae can also be derived for the pricing of swaptions or options on realized variance (see [32]). We will not work with swaptions and volatility swaps in this paper; we have only introduced the variance swap rate because it is relevant in evaluating the VIX and is hence relevant in the pricing of VIX options.

3.1.1 Relationship between the Variance Swaps, the VIX and the Log Contract

Let VIX_t denote the VIX index at time t (in hundredths of a decimal). The CBOE's VIX index, as it was re-furbished in 2002, is a discretization of the formula [6, 7, 8, 22],

$$\text{VIX}_t = \sqrt{\frac{2e^{r\tau}}{\tau} \left(\int_0^{F_{t,t+\tau}} \frac{P_{t,t+\tau}(K)}{K^2} dK + \int_{F_{t,t+\tau}}^{\infty} \frac{C_{t,t+\tau}(K)}{K^2} dK \right)} \quad (4)$$

where $\tau = 30$ days, $F_{t,t+\tau} = \mathbb{E}_t e^{X_{t+\tau}}$, and where $P_{t,t+\tau}(K)$ and $C_{t,t+\tau}(K)$ are a put option and a call option with strike K and maturity $t + \tau$, respectively. Futures on the VIX have been trading since March of 2004, and were sufficiently popular that the CBOE introduced options on the VIX in February of 2006. Both instruments are liquid, and if read correctly can provide a gauge of market sentiments for the coming months. VIX options will be covered in a later section; in this brief sub-section we will cover the relationship between variances swaps and the VIX.

When X_t has no jumps, VIX_t^2 is equivalent to the 30 day variance swap rate. It was shown in [9] that Lévy jumps in the underlying make the 30 day variance swap rate equal to VIX_t^2 plus a jump premium. We can derive a similar result for the regime model of (2).

The price of a futures contract on the stock is $F_{t,T} = \mathbb{E}_t e^{X_T}$. The future and log-future processes satisfy the following SDEs:

$$\begin{aligned} \int_t^T \frac{1}{F_{s-,T}} dF_{s,T} &= \int_t^T f(\theta_s) \sqrt{Y_s} dW_s + \int_t^T (e^{-\lambda(\theta_s)J_s} - 1) dN_s - \delta\nu(\theta_{s-}) ds, \\ \log(F_{T,T}/F_{t,T}) &= \int_t^T \frac{1}{F_{s-,T}} dF_{s,T} - \frac{1}{2} \int_t^T f^2(\theta_s) Y_s ds - \int_t^T (e^{-\lambda(\theta_s)J_s} - 1 + \lambda(\theta_s) J_s) dN_s. \end{aligned}$$

After some algebra we see that quadratic variation can be replicated by a combination of the log-contract and the future contract:

$$\begin{aligned} \frac{[X]_T - [X]_t}{T-t} &= \frac{1}{T-t} \int_t^T f^2(\theta_s) Y_s ds + \frac{1}{T-t} \int_t^T \lambda^2(\theta_s) J_s^2 dN_s \\ &= \frac{-2}{T-t} \left\{ \log \left[\frac{F_{T,T}}{F_{t,T}} \right] - \int_t^T \frac{dF_{s,T}}{F_{s-,T}} + \int_t^T \left[e^{-\lambda(\theta_s)J_s} - 1 + \lambda(\theta_s)J_s - \frac{1}{2}\lambda^2(\theta_s)J_s^2 \right] dN_s \right\} \end{aligned} \quad (5)$$

Set $T = t + \tau$ with $\tau = 30$ days. Recognizing that $\text{VIX}_t^2 = \frac{-2}{\tau} \mathbb{E}_t \log(F_{t+\tau,t+\tau}/F_{t,t+\tau})$ (see [6, 7, 9]) and that $\int \frac{1}{F_{s-,T}} dF_{s,T}$ is a martingale, we have the jump-premium between the variance swap rate and the VIX by taking expectations of both sides of (5):

$$\begin{aligned} \text{VS}_{t,\tau} &= \text{VIX}_t^2 - \frac{2}{\tau} \mathbb{E}_t \left\{ \int_t^{t+\tau} \left(e^{-\lambda(\theta_s)J_s} - 1 + \lambda(\theta_s)J_s - \frac{1}{2}\lambda^2(\theta_s)J_s^2 \right) dN_s \right\} \\ &= \text{VIX}_t^2 + \frac{2\delta}{\tau} \sum_{n,m \neq n} [I(t; \tau)]_{\theta_t, n} \frac{\lambda^3(m)}{1 + \lambda(m)} Q_{nm}, \end{aligned}$$

where $\text{VS}_{t,\tau}$ is the variance swap rate from (3). Therefore, model (2) has the following VIX formula:

$$\text{VIX}_t = \sqrt{\text{VS}_{t,\tau} - \frac{2\delta}{\tau} \sum_{n,m \neq n} [I(t; \tau)]_{\theta_t, n} \frac{\lambda^3(m)}{1 + \lambda(m)} Q_{nm}}. \quad (6)$$

3.2 PIDE for Option Pricing

For times $t \in [0, T]$, the no arbitrage price of a European payoff $h(X_T, Y_T, \theta_T)$ is simply its discounted expectation under the risk-neutral measure \mathbb{P} . We write the option price P^δ as a function of its time to maturity $\tau = T - t$:

$$P^\delta(\tau, x, y, n) = e^{-r\tau} \mathbb{E}\{h(X_T, Y_T, \theta_T)|X_t = x, Y_t = y, \theta_t = n\}. \quad (7)$$

It satisfies the following PIDE:

$$\begin{aligned} (\mathcal{L}_n + \delta \mathcal{M}) P^\delta &= 0, \\ P^\delta|_{\tau=0} &= h(x, y, n), \end{aligned} \quad (8)$$

where \mathcal{L}_n is the pure-diffusion Heston operator in regime n :

$$\mathcal{L}_n = -\frac{\partial}{\partial \tau} + \frac{1}{2} f^2(n) y \left(\frac{\partial^2}{\partial x^2} - \frac{\partial}{\partial x} \right) + \rho \gamma f(n) y \frac{\partial^2}{\partial x \partial y} + \frac{\gamma^2 y}{2} \frac{\partial^2}{\partial y^2} + \kappa (\bar{Y} - y) \frac{\partial}{\partial y} + r \left(\frac{\partial}{\partial x} - \cdot \right),$$

and \mathcal{M} is the integral operator from the jumps,

$$\mathcal{M} P^\delta(\tau, x, y, n) = \sum_{m \neq n} Q_{nm} \left(\int_0^\infty P^\delta(\tau, x - \lambda(m)u, y, m) e^{-u} du - P^\delta(\tau, x, y, n) \right) - \nu(n) \frac{\partial}{\partial x} P^\delta(\tau, x, y, n).$$

The expectation (7) can of course be approximated using Monte Carlo, and there are reliable methods for simulating Markov processes like the one under consideration. However, Monte Carlo can be slow. It is also possible to solve (8) numerically (e.g. finite element methods), but it also may take a lot of computation time. However, the expansion that we derive for equity options is relatively fast for computing and is a good approximation when δ is small (e.g. $\delta = .01$).

4 Slow Regime Shift Expansion around the Heston Model

This section will use an asymptotic expansion to approximate the solution to equation (8) for various European payoffs. We expand the solution in powers of δ , apply the PIDE, and match powers in a way that exploits explicit solutions in the simpler Heston model, which will be the base-term of the expansion. This basis for expansion was initiated in [20] with a fast mean-reverting and correlated amplification factor on top of Heston, where it was shown that the Fourier transform of the first correction term in the series could be computed semi-explicitly in terms of the Heston Fourier expression. Here, the extension is slow, uncorrelated regime shifts which will be needed to reproduce VIX implied volatility skews.

We start by expressing the price P^δ in powers of δ ,

$$P^\delta = P_0 + \delta P_1 + \delta^2 P_2 + \dots \quad (9)$$

and we look for terms P_0 and P_1 etc. that do not depend on δ . Inserting the δ -expansion into (8), we get the following system of equations for P_0 and P_1 .

Definition 4.1. *The zero-order term is the Heston model's price (with θ_t frozen at n) of the European option:*

$$\mathcal{L}_n P_0 = 0, \quad \text{with} \quad P_0(0, x, y, n) = h(x, y, n). \quad (10)$$

The δ -correction is the solution to the inhomogeneous equation

$$\mathcal{L}_n P_1 = -\mathcal{M}P_0, \quad \text{with} \quad P_1(0, x, y, n) = 0. \quad (11)$$

For European call options and for volatility options, the zero-order term P_0 is priced under a Heston model and can be computed using a Fourier transform. A similar expansion could also be derived for the model in [32] where there are also jumps in Y 's SDE, so long as the intensity of jumps is of order δ . We will use the notation of [20, 21], mainly because they have derived the pricing formula using a Green's function (we call it \widehat{G}). The Green's function is a way of expressing the solution of (8) for general payoff function $h(x)$.

4.1 Stock Options

Consider the class of payoffs where the function h does not depend on y ,

$$P^\delta(\tau, x, y, n) = e^{-r\tau} \mathbb{E}\{h(X_T, \theta_T) | X_t = x, Y_t = y, \theta_t = n\}.$$

The explicit formula in [25] is for the Fourier transform of the European call option under a Heston model, but can be extended to obtain affine formulae for models with jumps [2, 28]. In this section we introduce an expansion that serves for a generalized class of models with jumps and regime-change.

For the option price P^δ , the Fourier transform (and its inverse) are defined as

$$\widehat{P}^\delta(\tau, \omega, y, n) = \int_{\mathbb{R}} e^{i\omega q(\tau, x)} P^\delta(\tau, x, y, n) dx \quad \forall \omega \in \mathbb{C}, \quad (12)$$

$$P^\delta(\tau, x, y, n) = \frac{1}{2\pi} \int_{ic-\infty}^{ic+\infty} e^{-i\omega q(\tau, x)} \widehat{P}^\delta(\tau, \omega, y, n) d\omega \quad \text{for some } c \in \mathbb{R}, \quad (13)$$

where $q(\tau, x) = r\tau + x$. Using the expansion (9), the Fourier transform becomes a sum of Fourier transforms:

$$\widehat{P}^\delta(\tau, \omega, y, n) = \widehat{P}_0(\tau, \omega, y, n) + \delta \widehat{P}_1(\tau, \omega, y, n) + \dots,$$

and so P^δ can be reconstructed from the Fourier transforms of the expansion terms. We solve for each Fourier transform separately and then invert.

4.1.1 The Zero-Order Term

Applying the Fourier transform to (10), we see that $\widehat{P}_0(\tau, \omega, y, n)$ satisfies the following PDE

$$\widehat{\mathcal{L}}_n \widehat{P}_0(\tau, \omega, y, n) = 0,$$

where

$$\widehat{\mathcal{L}}_n = -\frac{\partial}{\partial \tau} + \frac{1}{2}\gamma^2 y \frac{\partial^2}{\partial y^2} + (\kappa \bar{Y} - \beta_n(\omega)y) \frac{\partial}{\partial y} + \alpha_n(\omega)y \cdot,$$

and

$$\alpha_n(\omega) = \frac{1}{2}f^2(n)(i\omega - \omega^2), \quad \beta_n(\omega) = \kappa + i\rho\omega\gamma f(n). \quad (14)$$

The initial condition is

$$\widehat{P}_0(0, \omega, y, n) = \widehat{h}_n(\omega) := \int e^{i\omega x} h(x, n) dx.$$

The formula for $\widehat{P}_0(\tau, \omega, y, n)$ is given in [20, 22] in terms of \widehat{G}_n , the Fourier transform of the Green's function, which is the exponential of an affine function of y :

$$\widehat{P}_0(\tau, \omega, y, n) = \widehat{G}_n(\tau, \omega, y) \widehat{h}_n(\omega), \quad (15)$$

$$\widehat{G}_n(\tau, \omega, y) = \exp(C_n(\tau, \omega) + yD_n(\tau, \omega)), \quad (16)$$

$$C_n(\tau, \omega) = \frac{\kappa \bar{Y}}{\gamma^2} \left((\beta_n(\omega) - d_n(\omega))\tau - 2 \log \left(\frac{1 - e^{-\tau d_n(\omega)} / g_n(\omega)}{1 - 1/g_n(\omega)} \right) \right), \quad (17)$$

$$D_n(\tau, \omega) = \frac{\beta_n(\omega) - d_n(\omega)}{\gamma^2} \left(\frac{1 - e^{-\tau d_n(\omega)}}{1 - e^{-\tau d_n(\omega)} / g_n(\omega)} \right), \quad (18)$$

$$d_n(\omega) = \sqrt{\beta_n^2(\omega) - 2\gamma^2 \alpha_n(\omega)}, \quad (19)$$

$$g_n(\omega) = \frac{\beta_n(\omega) + d_n(\omega)}{\beta_n(\omega) - d_n(\omega)}, \quad (20)$$

where it should be pointed out that equations (17) and (18) have been written with a complex conjugation that avoids branch cuts in the path of integration. To obtain the Heston model price of the option, the integral can be inverted with the following formula:

$$P_0(\tau, x, y, n) = \frac{e^{-r\tau}}{2\pi} \int_{ic-\infty}^{ic+\infty} \operatorname{Re} \left(e^{-i\omega q(\tau, x)} \widehat{h}_n(\omega) \widehat{G}_n(\tau, \omega, y) \right) d\omega. \quad (21)$$

The integration in (21) could be done over the positive real line only, but a shift of the domain of integration needs to be done (see [28]). Fourier transforms of non-smooth payoff functions are addressed in [28] and will dictate the imaginary component c in equations (13) and (21). Such payoffs include the European call, $h(x) = (e^x - K)^+$, for which it is required to take $c > 1$.

4.1.2 The δ -Correction

Applying the Fourier transform to equation (11), we see that the order- δ correction satisfies a PDE,

$$\begin{aligned}\widehat{\mathcal{L}}_n \widehat{P}_1(\tau, \omega, y, n) &= - \int e^{i\omega q(\tau, x)} \mathcal{M} P_0(\tau, x, y, n) dx \\ &= - \left(\sum_{m \neq n} Q_{nm} \frac{\widehat{P}_0(\tau, \omega, y, m)}{1 - i\omega \lambda(m)} + (Q_{nn} + \nu(n)i\omega) \widehat{P}_0(\tau, \omega, y, n) \right) \\ &= - \sum_{m=1}^3 \widehat{\mathcal{M}}_{nm} \widehat{P}_0(\tau, \omega, y, m),\end{aligned}\tag{22}$$

where matrix operator $\widehat{\mathcal{M}}$ is given by

$$\widehat{\mathcal{M}}_{nm} = Q_{nm} \frac{1 - i\omega \lambda(m) \mathbb{1}_{[m=n]}}{1 - i\omega \lambda(m)} + i\omega \nu(n) \mathbb{1}_{[m=n]}. \tag{23}$$

In general, the operators $\widehat{\mathcal{M}}$ and $\widehat{\mathcal{L}}_n$ do not commute, so we cannot write a solution of the form in [21] (that is, $\widehat{P}_1 \neq \tau \widehat{\mathcal{M}} \widehat{P}_0$). However, the solution to (22) can be written as a mixture in the regime variable of \widehat{P}_0 's:

Proposition 4.1. *The δ -correction is,*

$$\widehat{P}_1(\tau, \omega, y, n) = \sum_{m=1}^3 \widehat{\mathcal{M}}_{nm} \widehat{P}_0(\tau, \omega, y, m) \int_0^\tau a_{nm}(\tau, u, \omega, y) du, \tag{24}$$

where for any $u \leq \tau$, we define

$$a_{nm}(\tau, u, \omega, y) = \exp(\psi_{nm}(\tau, u, \omega) + y \chi_{nm}(\tau, u, \omega)), \tag{25}$$

and ψ_{nm} and χ_{nm} solve the ODEs

$$\begin{aligned}\frac{\partial}{\partial \tau} \chi_{nm}(\tau, u, \omega) &= \frac{1}{2} \gamma^2 \chi_{nm}^2 - c_{nm}(\tau, \omega) \chi_{nm} + H_{nm}(\tau), \quad \text{with } \chi_{nm}(u, u, \omega) = 0, \\ \frac{\partial}{\partial \tau} \psi_{nm}(\tau, u, \omega) &= \kappa \bar{Y} \chi_{nm}(\tau, u, \omega), \quad \text{with } \psi_{nm}(u, u, \omega) = 0,\end{aligned}\tag{26}$$

with

$$c_{nm}(\tau, \omega) = \beta_n(\omega) + \gamma^2 D_m(\tau, \omega), \quad H_{nm}(\tau, \omega) = -(\beta_n(\omega) - \beta_m(\omega)) D_m(\tau, \omega) + (\alpha_n(\omega) - \alpha_m(\omega)). \tag{27}$$

Proof. We look for a solution to (22) of the form

$$\widehat{P}_1(\tau, \omega, y, n) = \sum_{m=1}^3 b_{nm}(\tau, y, \omega) \widehat{\mathcal{M}}_{nm} \widehat{P}_0(\tau, \omega, y, m), \tag{28}$$

for $b_{nm}(\tau, y, \omega)$ to be found. Since

$$\widehat{\mathcal{L}}_n = \widehat{\mathcal{L}}_m - (\beta_n(\omega) - \beta_m(\omega)) y \frac{\partial}{\partial y} + (\alpha_n(\omega) - \alpha_m(\omega)) y \cdot,$$

and $\widehat{\mathcal{L}}_m \widehat{P}_0(\tau, \omega, y, m) = 0$, we compute that

$$\widehat{\mathcal{L}}_n \widehat{P}_0(\tau, \omega, y, m) = H_{nm}(\tau, \omega) y \widehat{P}_0(\tau, \omega, y, m),$$

where $H_{nm}(\tau, \omega)$ is given in (27), and we have used that $\frac{\partial}{\partial y} \widehat{P}_0(\tau, \omega, y, m) = D_m(\tau, \omega) \widehat{P}_0(\tau, \omega, y, m)$. Then

$$\widehat{\mathcal{L}}_n b_{nm}(\tau, y, \omega) \widehat{\mathcal{M}}_{nm} \widehat{P}_0(\tau, \omega, y, m) = \widehat{\mathcal{M}}_{nm} \widehat{P}_0(\tau, \omega, y, m) \widehat{L}_{nm} b_{nm}(\tau, y, \omega),$$

where

$$\widehat{L}_{nm} = -\frac{\partial}{\partial \tau} + \frac{1}{2} \gamma^2 y \frac{\partial^2}{\partial y^2} + (\kappa \bar{Y} - c_{nm}(\tau, \omega) y) \frac{\partial}{\partial y} + H_{nm}(\tau, \omega) y,$$

and $c_{nm}(\tau, \omega)$ is given in (27). Consequently, (28) satisfies (22) if for each (n, m) , $\widehat{L}_{nm} b_{nm} = -1$ with $b_{nm}(0, y) = 0$. This is solved by

$$b_{nm}(\tau, y, \omega) = \int_0^\tau a_{nm}(\tau, u, \omega, y) du,$$

where for $\tau \geq u$, $a_{nm}(\tau, u, \omega, y)$ solves

$$\widehat{\mathcal{L}}_n a_{nm}(\tau, u, \omega, y) = 0, \quad a_{nm}(u, u, \omega, y) = 1.$$

This is a CIR-type computation, and the solution is given by (25). \square

The expression in (25) is well-defined for all $\omega < \infty$, but it needs to be verified that the expression in (24) is integrable over ω from $-\infty$ to ∞ . It turns out that the Riccati equations in (26) are not well behaved for large $|\omega_r|$ (if $f(n) - f(m) < 0$), but exponential decay of $\widehat{P}_0(\tau, \omega, y, m)$ will dampen any solutions that diverge.

4.2 VIX Options

In this section we consider payoffs which are functions of the volatility processes only (i.e. on θ_T and Y_T). Payoffs of this type include the variance swap rate of (3) and the VIX of equation (6). It should be pointed out that options on realized variance/volatility are not covered in this section because they're dependent on the path of X ; they are more like Asian options and should be priced with an expansion similar to the stock option expansion of Section 4.1, but with an additional state variable for the accumulated variance or volatility (see [27, 32]).

Options on the volatility process have payoffs of the form $h(y, n)$. Since θ_t and Y_t do not depend on X_t , neither will the price of such a claim. Therefore, all that is needed is to compute the transition density of the volatility processes, and the option price can be written as an integral over this density. Since θ and Y are independent, we have

$$\begin{aligned} P^\delta(\tau, y, n) &= e^{-r\tau} \mathbb{E}\{h(Y_T, \theta_T) | Y_t = y, \theta_t = n\} \\ &= e^{-r\tau} \sum_m \int h(z, m) p_0(\tau, z, y) \mathbb{P}(\theta_T = m | \theta_t = n) dy, \end{aligned}$$

where $p_0(\tau, z, y) = \frac{d}{dz} \mathbb{P}(Y_T \leq z | Y_t = y)$. The Fourier transform in z of the density p_0 is

$$\widehat{p}_0(\tau, \omega, y) = \int e^{i\omega z} p_0(\tau, z, y) dz,$$

which satisfies a backward equation

$$\begin{aligned} \left(-\frac{\partial}{\partial \tau} + \frac{1}{2}\gamma^2 y \frac{\partial^2}{\partial y^2} + \kappa(\bar{Y} - y) \frac{\partial}{\partial y} \right) \hat{p}_0 &= 0, \\ \hat{p}_0 |_{\tau=0} &= e^{i\omega y}. \end{aligned} \quad (29)$$

The solution to (29) is used to price VIX options in [32], but affine formulae and solutions of Riccati equations for the Fourier transforms of more general classes of Markov processes are given in [17, 18]. Explicitly, \hat{p}_0 is given by

$$\begin{aligned} \hat{p}_0(\tau, \omega, y) &= \exp(A(\tau, \omega) + yB(\tau, \omega)), \\ A(\tau, \omega) &= -\frac{2\bar{Y}\kappa}{\gamma^2} \log\left(-\frac{i\omega\gamma^2}{2\kappa}(1 - e^{-\kappa\tau}) + 1\right), \\ B(\tau, \omega) &= \frac{i\omega e^{-\kappa\tau}}{\frac{-i\omega\gamma^2}{2\kappa}(1 - e^{-\kappa\tau}) + 1}, \end{aligned} \quad (30)$$

for any $\omega \in \mathbb{C}$. Finally we can easily compute the matrix exponential of Q to obtain the Markov chain transition probability,

$$P(\theta_T = m | \theta_t = n) = \left[e^{\delta\tau Q} \right]_{n,m}.$$

Using the formula from Section 3.1.1, the payoff for a VIX option is written as a function of y and n ,

$$h(y, n) = \left(\sqrt{\text{VS}_{\tau_{vix}}(y, n) - \frac{2\delta}{\tau_{vix}} \left(\sum_{n'} [I(0, \tau_{vix})]_{n, n'} \sum_{m \neq n'} \frac{\lambda^3(m)}{1 + \lambda(m)} Q_{n' m} \right)} - K \right)^+, \quad (31)$$

where $\tau_{vix} = \frac{30}{365}$ and $\text{VS}_{\tau_{vix}}(y, n)$ is the variance swap rate (as explained in Section 3.1). Hence, the VIX option is given by

$$\begin{aligned} P^\delta(\tau, y, n) &= e^{-r\tau} \mathbb{E}\{(VIX_T - K)^+ | Y_t = y, \theta_t = n\} \\ &= \frac{e^{-r\tau}}{\pi} \sum_m [e^{\tau Q}]_{n, m} \int_0^\infty h(y', m) \mathbb{P}(Y_T \in dy' | Y_t = y) \\ &= \frac{e^{-r\tau}}{\pi} \sum_m [e^{\tau Q}]_{n, m} \int_0^\infty h(y', m) \int_0^\infty \text{Re} \left(e^{-i\omega y'} \hat{p}_0(\tau, \omega, y) \right) d\omega dy'. \end{aligned} \quad (32)$$

Figure 4 is a comparison of a VIX implied volatility from the Heston model versus the implied volatility of model (2) computed using the probability density of (30) and the formula of (32). Notice that implied volatility of the basic Heston model is not upward sloping, whereas having regime change makes the implied volatility upward sloping like the implied volatility seen from data in Figure 3 of Section 2.2.

5 Numerical Methods & Calibration

We now turn our attention to options data to see if model (2) has the potential to capture market dynamics. First we look at SPX and VIX options on July 27th, 2012, with expiries in August, September, October and November. Later in Section 5.2.3, we look at VIX options from the crisis of the Fall 2008 and compare the calibrated parameters to those of the non-crisis VIX options of February 2011.

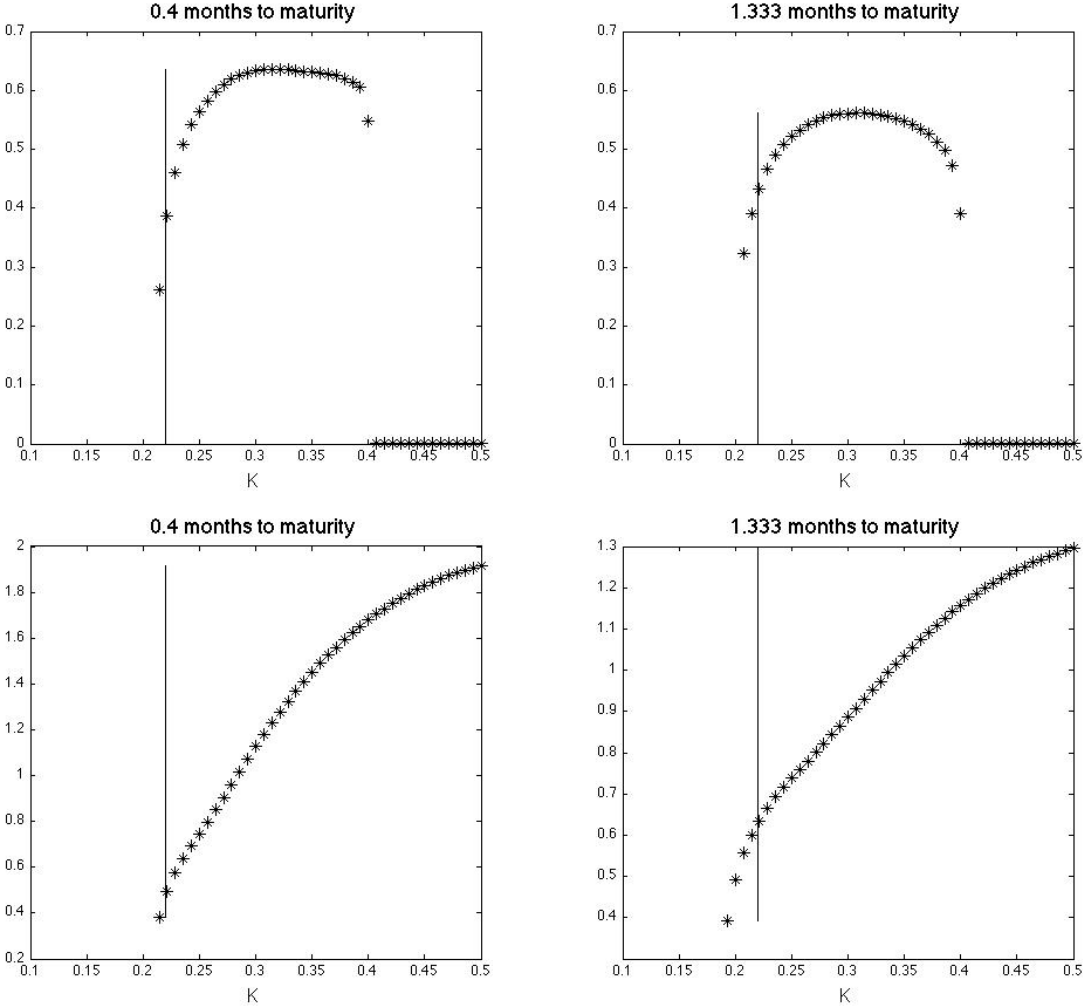


Figure 4: **Top:** Implied volatilities of VIX options for a basic Heston model (without regime change). **Bottom:** Implied volatility of VIX options for model (2) computed using (32).

Given call options $P^{data}(\tau; K_\ell)$ with strike K_1, K_2, \dots, K_L , the calibration problem is

$$\min \sum_{\ell=1}^L \left(P^\delta(\tau, X_t, Y_t, \theta_t; K_\ell) - P^{data}(\tau; K_\ell) \right)^2, \quad (33)$$

where the minimization occurs over the parameter space of $(\kappa, \gamma, \bar{Y}, \rho, \lambda, Q, f)$. Another performance measure that we shall use is absolute-relative error:

$$\text{rel-err.} = \frac{1}{L} \sum_{\ell=1}^L \frac{|P^\delta(\tau, X_t, Y_t, \theta_t; K_\ell) - P^{data}(\tau; K_\ell)|}{P^{data}(\tau; K_\ell)}. \quad (34)$$

The parameters $(\kappa, \gamma, \bar{y}, \rho)$ can capture the basic qualities of the implied volatility smile for SPX options, but the addition of jumps will significantly improve the fit, particularly for options with short time-to-maturity. For VIX options, the inclusion of Q and f is essential, as regime-change in the underlying's volatility is what drives the market for out-of-the-money VIX calls.

In Sections 5.1 and 5.2, model (2) is fit to the data in a number of different ways: the non-jump and non-regimed Heston model to the SPX options; the full model to the SPX options; the full model to the VIX options. We find that the higher degree of explanatory power allows for a better fit to SPX options, and that significant regime-change allows for accurate calibration to VIX options, which could not be priced by the basic Heston model.

5.1 Calibration of SPX Call Options

Call options on the SPX index have a payoff $h(x) = (e^x - K)^+$. As we mentioned in Section 4.1.1 (see [20] or [28, page 37]), it is required that $\text{Im}(\omega) = c > 1$ in order for the Fourier transform of h to exist, in which case we have

$$\hat{h}(\omega) = \int e^{i\omega x} (e^x - K)^+ dx = \frac{K^{1+i\omega}}{i\omega - \omega^2}.$$

Setting $\omega = \omega_r + ic$, we apply the formula of (21) for \hat{P}_0 to get the zero-order term,

$$P_0(\tau, x, y, n) = \frac{e^{-r\tau}}{2\pi} \int_{-\infty}^{\infty} \text{Re} \left(e^{-i\omega(r\tau+x)} \hat{G}_n(\tau, \omega, y, n) \frac{K^{1+i\omega}}{i\omega - \omega^2} \right) d\omega_r,$$

which can be computed numerically with Gaussian quadrature, and fit to the SPX options with a nonlinear least squares algorithm. The fits obtained using Matlab's 'quadgk' and 'lsqcurvefit' functions are shown in Figure 5 and the estimated parameters are listed in Table 1. The function 'lsqcurve' seeks parameters to minimize the absolute error of (33). The upper-left plot of Figure 5 shows that the basic Heston

Maturity	Y_0	κ	\bar{Y}	$\gamma^2/(2\kappa\bar{Y})$	ρ	rel-err.
Aug	0.0001	9.99	0.1444	0.2427	-0.62	0.1514
Sep	0.0116	9.77	0.0582	0.3014	-0.59	0.0033
Oct	0.0150	8.39	0.0456	0.4605	-0.71	0.0109
Nov	0.0161	5.61	0.0516	0.5472	-0.70	0.0007

Table 1: For the SPX options data, these are the parameter estimates for the Heston model with no jumps (i.e. $f \equiv 1$, $Q \equiv 0$, $\lambda \equiv 0$).

model cannot fit the implied volatility of low-strike options with short time-to-maturity. This is a well-known weakness of the Heston model, and is one of the many reasons for the inclusion of jumps. It also an indication that the Heston model cannot price VIX or VIX options because these low-strike short-maturity options are highly-weighted in the CBOE's VIX formula.

5.1.1 Fit of the Jump Model to SPX Options Data

In this subsection, we calibrate to the SPX options and explain the procedure for fitting model (2) using the Fourier expansions terms \hat{P}_0 and \hat{P}_1 . By including the correction term \hat{P}_1 , there is significant improvement in the fits of implied volatility, most noticeably for the option with shortest time-to-maturity. In general, jump models are expected to have a better fit because they have a higher degree of explanatory power, and so it is to be expected that \hat{P}_1 will improve the fit. The parameter estimates and the fitted implied volatilities are shown in Table 2 and Figure 6, respectively.

To calibrate the model, we again used Matlab's 'quadgk' and 'lsqcurvefit' functions. Since δ and $f(2)$ are parameters that do not add extra explanatory power (because δ can be compensated by Q , and f can be compensated by Y_0 , \bar{Y} and γ), we take the following parameters as fixed: $\delta = .01$ and $f(2) = 1$.

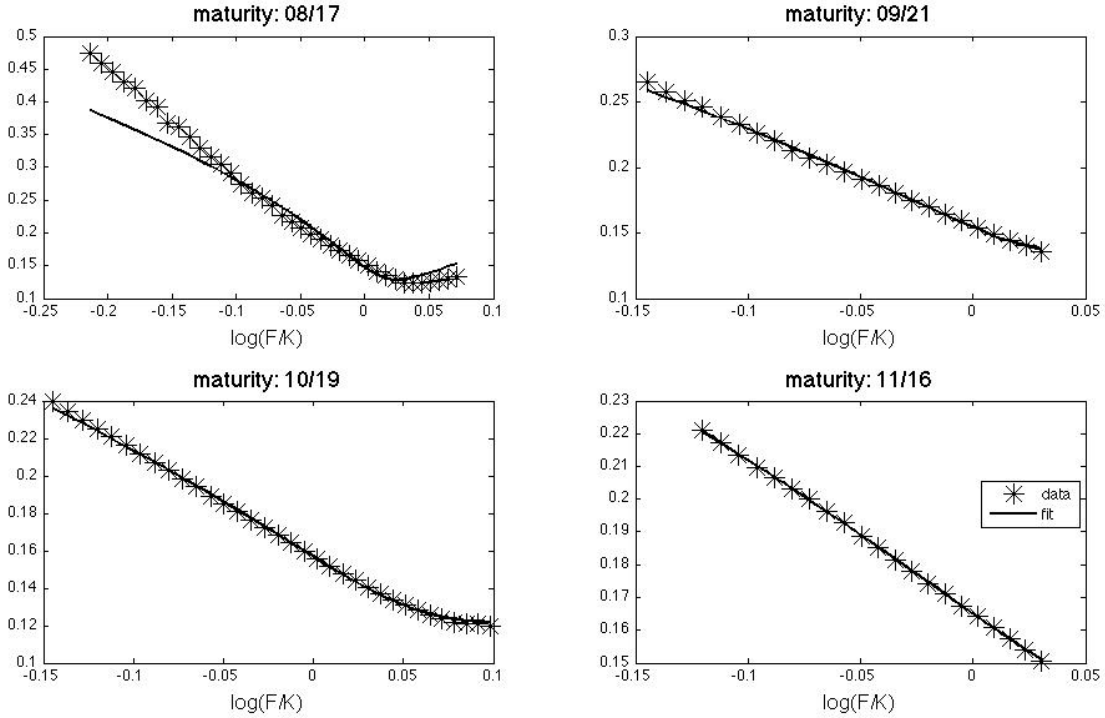


Figure 5: The implied volatilities of July 27th SPX options, alongside those of a fitted Heston model with no jumps (i.e. $f \equiv 1$, $Q \equiv 0$, and $\lambda \equiv 0$). The values of the other fitted parameters are given in Table 1.

Mat.	Y_0	κ	\bar{Y}	$\gamma^2/(2\kappa\bar{Y})$	ρ	$f(1)$	$f(3)$	Q_{21}	Q_{22}	Q_{23}	$\lambda(1)$	$\lambda(2)$	$\lambda(3)$	rel-err.
Aug	0.0109	4.49	0.0832	0.6085	-0.66	0.55	1.83	1.0	-28.1	27.1	-0.30	0.00	0.25	0.0385
Sep	0.0116	3.31	0.0555	0.9837	-0.65	1.73	2.13	3.2	-28.5	25.4	-0.05	-0.06	0.20	0.0009
Oct	0.0079	3.19	0.0679	0.9783	-0.75	0.59	4.98	3.1	-6.2	3.1	-0.08	0.14	0.82	0.0024
Nov	0.0180	2.71	0.0440	0.9900	-0.83	0.88	4.98	8.0	-18.0	10.0	-0.09	0.75	0.22	0.0012

Table 2: For the SPX options data, these are the parameter estimates for model (2), $\theta_0 = 2$, $f(2) = 1$, and $\delta = .01$.

We also take $\theta_0 = 2$ since this is the mid-level regime and July 27th could be considered a day with volatility at an *average* level. Depending on the time-to-maturity, the optimization took between 5 and 15 iterations to arrive at the parameter estimates in Table 2. The gradient-descent algorithm of lsqcurvefit will depend on the initial guess of the parameters, but we found the calibration to be fairly robust to this initial guess. Alternatively, one could look ahead to the parameter estimates in Table 3 and use them as an initial guess.

5.2 Calibration of VIX Options

Calibration of model (2) to VIX options is much faster than calibrating to SPX options; it takes on the order of 1 minute to generate the estimates and plots in Table 3 and Figure 7, respectively. Therefore, it makes sense to first calibrate to VIX options, and then use these parameters to fit the SPX options, and then re-adjust if needed. This section will explore the calibration of the model to the VIX options and make comparisons of the VIX options' parameters to those of the SPX options.

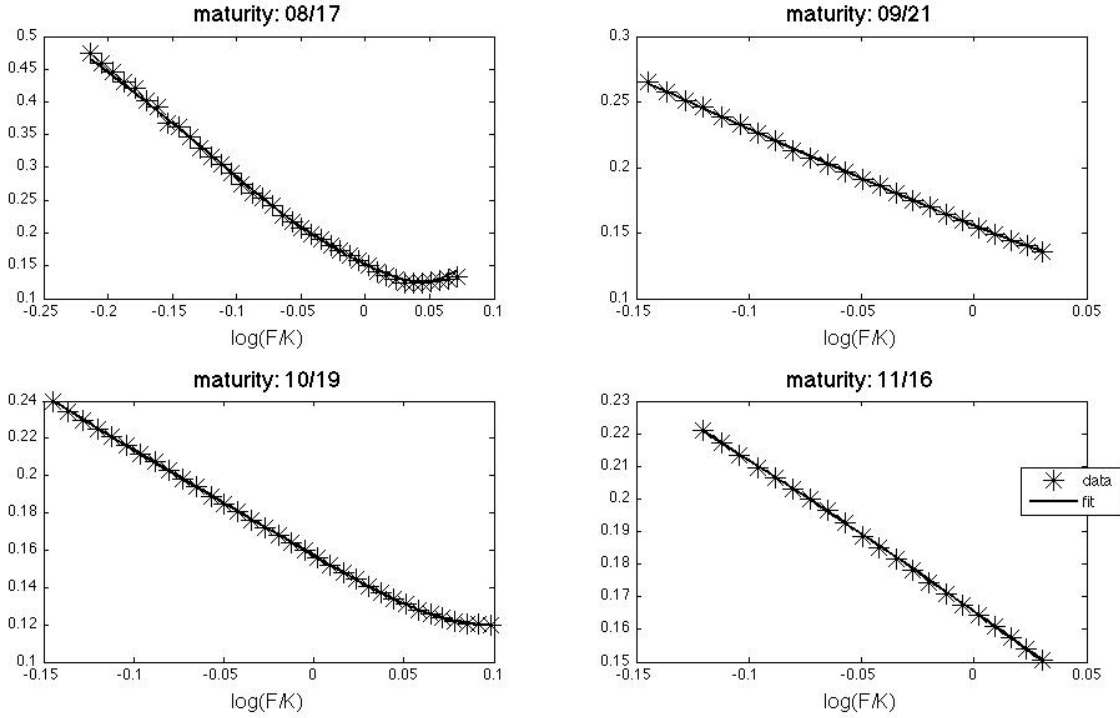


Figure 6: The implied volatilities of July 27th SPX options, alongside those of a fitted Heston model **with jumps** (i.e. $\lambda \neq 0$). The fitted parameters values are given in Table 2. Notice the improvement in the shortest time-to-maturity compared to the fit of the same option in Figure 5.

5.2.1 Numerical Computation of Y 's Transition Density using Laguerre Polynomials

For $\alpha \geq 0$, let Z_t be a square-root process such that

$$dZ_t = (1 + \alpha - Z_t)dt + \sqrt{2Z_t} dB_t$$

where B_t is the same Brownian motion as in (2). The transition density for this process can be written in terms of an infinite series of Laguerre polynomials (see [21, 29]):

$$\frac{d}{dz'} \mathbb{P}(Z_t \leq z' | Z_t = z) = \mu^\alpha(z') \sum_{\ell=0}^{\infty} L_\ell^\alpha(z') L_\ell^\alpha(z) e^{-\ell(T-t)} \quad \forall t \leq T \text{ and } \forall z, z' \in \mathbb{R}^+,$$

where $\mu^\alpha(z) = \frac{z^\alpha e^{-z}}{\Gamma(\alpha+1)}$, L_ℓ^α denotes the ℓ^{th} generalized Laguerre polynomial

$$L_\ell^\alpha(z) = e^z z^{-(\ell+\alpha)} \frac{d^\ell}{dz^\ell} \left(e^{-z} z^{\ell+\alpha} \right) \left(\frac{\ell! \Gamma(\alpha+1)}{\Gamma(\ell+\alpha+1)} \right)^{-1/2}, \quad (35)$$

and Γ denotes the Gamma function. These polynomials form an orthonormal basis with respect to μ^α ,

$$\int L_\ell^\alpha(z) L_{\ell'}^\alpha(z) \mu^\alpha(z) dz = \mathbb{1}_{[\ell=\ell']}.$$

Furthermore, for $\alpha = \frac{2\kappa\bar{Y}}{\gamma^2} - 1$, it can be verified that

$$Y_t \stackrel{d}{=} \frac{\gamma^2}{2\kappa} Z_{\kappa t},$$

and so the transition density in (32) can be well-approximated with the first 16 orthonormal polynomials,

$$\begin{aligned} \frac{d}{dy'} \mathbb{P}(Y_T \leq y' | Y_t = y) &= \frac{d}{dy'} \mathbb{P}\left(Z_{\kappa(T-t)} \leq \frac{2\kappa}{\gamma^2} y' \middle| Z_0 = \frac{2\kappa}{\gamma^2} y\right) \\ &\approx \frac{2\kappa}{\gamma^2} \mu^\alpha \left(\frac{2\kappa}{\gamma^2} y'\right) \sum_{\ell=0}^{15} L_\ell^\alpha \left(\frac{2\kappa}{\gamma^2} y'\right) L_\ell^\alpha \left(\frac{2\kappa}{\gamma^2} y\right) e^{-\ell\kappa(T-t)}. \end{aligned} \quad (36)$$

Taking 16 basis elements in (36) is equivalent to approximating the density with a 15-degree polynomial, which is a very good approximation provided that y is not far into the tail of Y 's probability distribution. The approximation in (36) is faster and more stable than a quadrature approximation of (32), and so we will use this formula when calibrating to the VIX options data.

5.2.2 Fit of Jump Model to VIX Options Data

In calibrating model (2) to VIX options, the choice of parameters $(f(1), f(3))$ is crucial because they impact the volatility process $\sigma_t = f(\theta_t)\sqrt{Y_t}$, allowing significant probability mass outside the range of the typical square-root process. The implied volatility fits are shown in Figure 7 and the estimated parameters in Table 3. From the figure it is clear that we have managed to price out-of-the-money VIX call options

mat.	Y_0	κ	\bar{Y}	$\gamma^2/(2\bar{Y}\kappa)$	$f(1)$	$f(3)$	Q_{21}	Q_{22}	Q_{23}	$\lambda(1)$	$\lambda(2)$	$\lambda(3)$	rel-err.
Aug	0.0180	8.19	0.0357	0.9894	1.0	3.0	15.1	-38.2	23.2	-0.060	0.041	0.037	0.1463
Sep	0.0115	4.72	0.0454	0.9893	2.0	3.9	15.3	-27.7	12.4	-0.060	-0.000	0.098	0.0458
Oct	0.0100	2.46	0.0832	0.9891	0.5	4.6	15.0	-22.4	7.4	-0.002	0.000	0.000	0.0108
Nov	0.0100	1.86	0.0994	0.9871	0.6	4.7	15.0	-19.2	4.2	-0.007	-0.000	-0.004	0.0330

Table 3: For the VIX options data, these are the parameter estimates for model (2), $\theta_0 = 2$, $\delta = .01$, $f(2) = 1$.

that were previously beyond the scope of the Heston model, and so we can conclude that the addition of volatility regime-change has made a difference.

The parameters in Table 3 differ from those in Table 2, some by a small relative amount, some by more, so it is hard to determine the degree of consistency between the two markets. However if we take the VIX option-calibrated parameters and compute the model's SPX option prices, then we see in Figure 8 that there is a distinct and striking mismatch, particularly for options with shorter time-to-maturity.

To determine if there was a possible fit that matches both markets, we did a simultaneous calibration and found the mismatch to remain (see Table 4 and Figure 9). A similar mismatch in prices is also found independently in [33], wherein several stochastic volatility models were tested and found to be misspecified when fit to both S&P 500 and VIX data, and also in [12] where it was found that the information content of the SPX was not identical to that of the VIX.

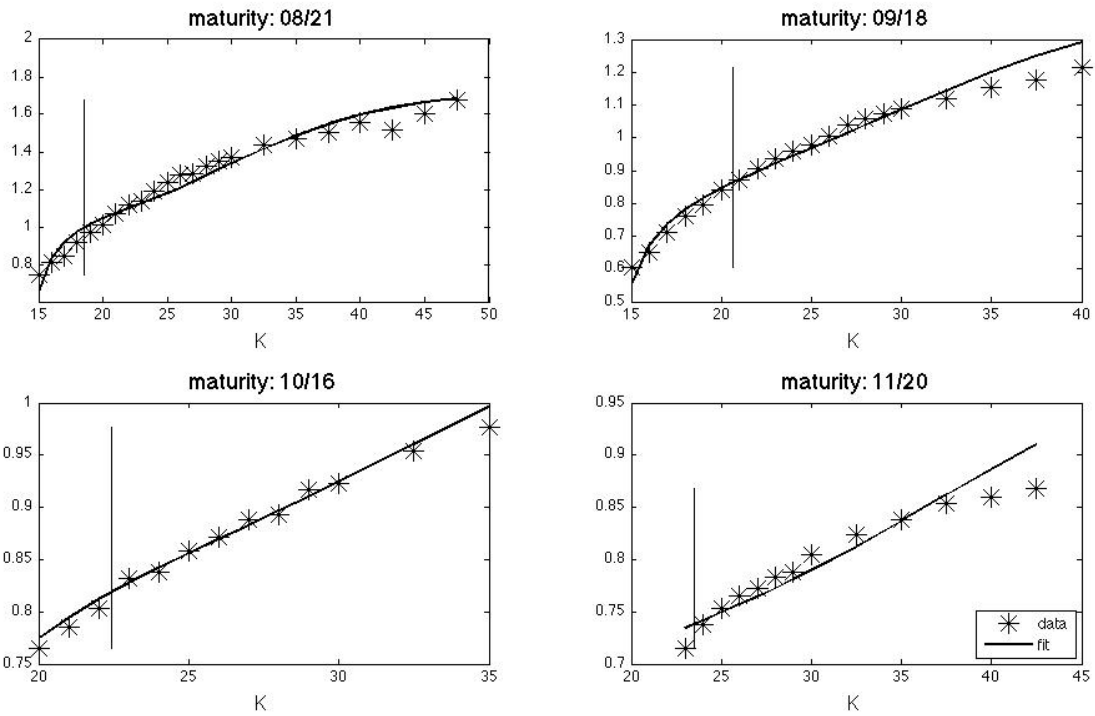


Figure 7: The implied volatilities of July 27th VIX options, alongside those of a fitted Heston with jumps. The fitted parameter values are given in Table 3. The vertical line marks the VIX futures price on the date of maturity.

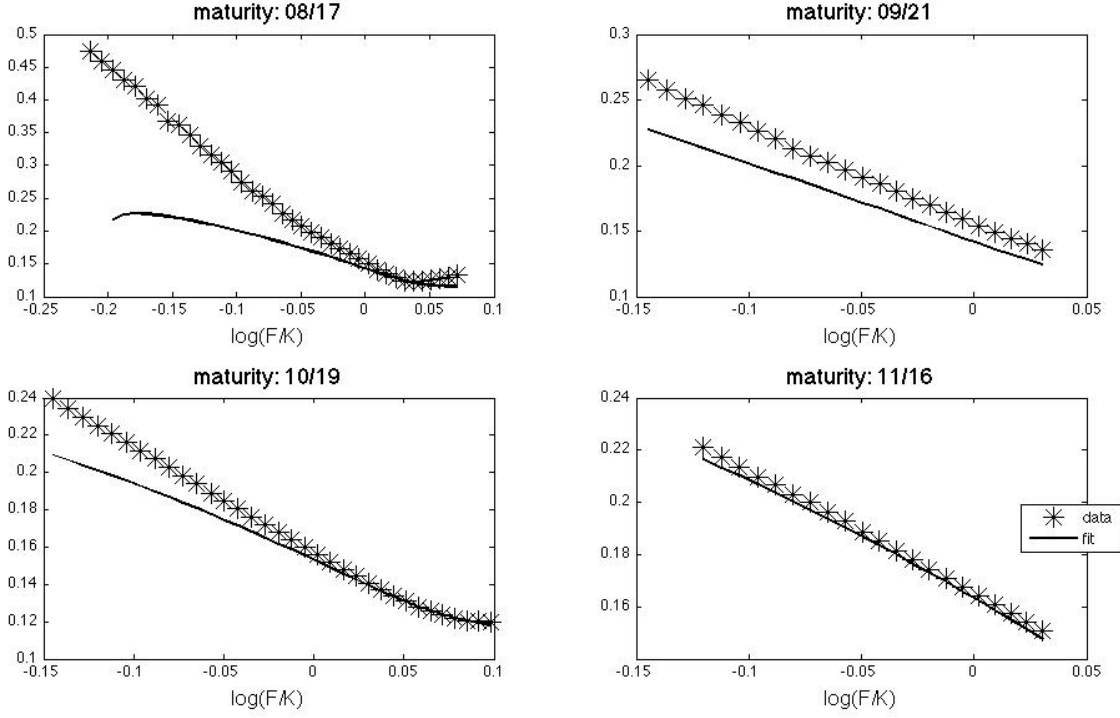


Figure 8: The implied volatilities of July 27th SPX options, alongside those of a Heston with jumps calculated using the parameter estimates of Table 3 (i.e. the parameters estimated from the VIX options data –not the SPX data).

Mat.	Y_0	κ	\bar{Y}	$\frac{\gamma^2}{2\kappa Y}$	ρ	$f(1)$	$f(3)$	Q_{21}	Q_{22}	Q_{23}	$\lambda(1)$	$\lambda(2)$	$\lambda(3)$	rel-err. SPX	rel-err. VIX.
Aug	0.03	8.58	0.0299	0.99	-0.67	0.82	3.02	14.6	-41.0	26.4	-0.01	0.04	0.09	0.06	0.16
Sep	0.01	4.72	0.0452	0.99	-0.65	1.98	3.90	15.3	-27.7	12.4	-0.06	-0.00	0.10	0.03	0.13
Oct	0.01	2.46	0.0813	0.99	-0.75	0.53	4.55	15.0	-22.4	7.3	-0.00	0.00	0.00	0.05	0.11
Nov	0.01	1.86	0.0993	0.99	-0.84	0.60	4.74	15.3	-19.6	4.2	-0.00	-0.07	0.01	0.01	0.03

Table 4: A simultaneous fit to both the VIX and SPX options, $\theta_0 = 2$, $f(2) = 1$, and $\delta = .01$. Both the relative error of the fit for SPX options and VIX options has increased from this reported in Tables 2 and 3, respectively.

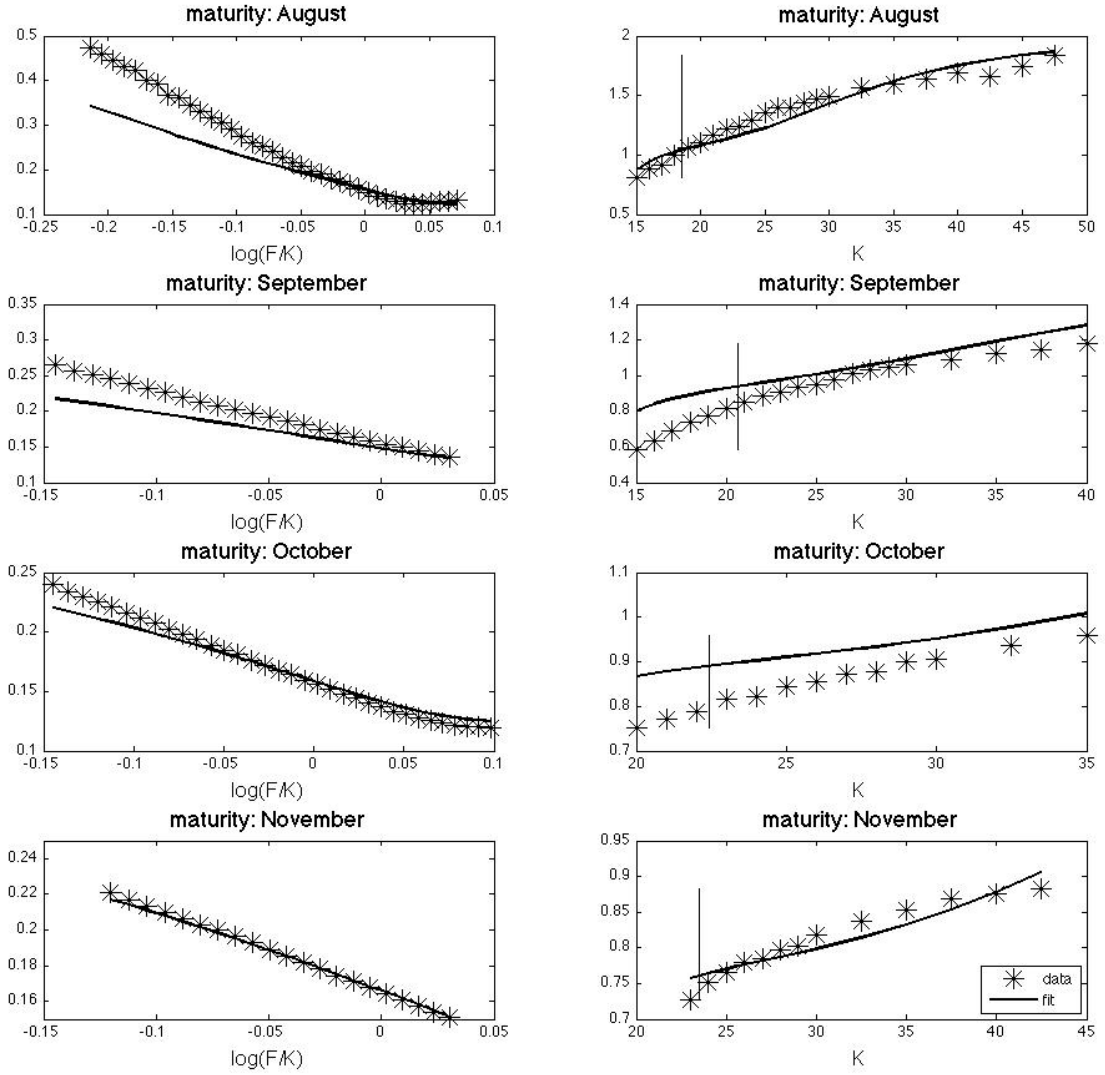


Figure 9: The implied volatilities of July 27th SPX options (left column) and VIX options (right column), plotted alongside those of a fitted Heston with jumps. The fitted parameter values are given in Table 4. The vertical lines in the plots on the right mark the VIX futures price on the date of maturity.

It should be pointed out that we have only fit a narrow range of strikes for VIX call options. After cleaning the data of options that could be deemed illiquid because of low volume and/or little open interest, we were left with roughly 12 options for each maturity, namely, those options with strike near the money and those with strikes 10 points higher. If we were to fit the extremely low and extremely high strike options, we might find ourselves limited by only three regimes. Indeed, more regimes means more spreading-out of the probability mass, and thus might be effective in fitting **all** listed options. However, a model with too many regimes might be considered unfounded, as the clear explanation for using three distinct regimes can have a certain amount of appeal in practice (e.g. for the VIX tail hedge).

5.2.3 Comparison of VIX Parameters: Crisis vs. Post-Crisis Era

In this section, we compare VIX options data from the crisis of Fall 2008 to data from a non-crisis period. In both cases we calibrate to the most liquid options with the shortest time-to-maturity. For the crisis we consider the dates of October 8th through 16th of 2008. The VIX was at 57% on the 8th, and rose to a high of 80% on October 27th (and hit 80% again in November), and would not drop below 40% until January 2nd of 2009. For the non-crisis dates we consider February 4th through 14th of 2011, a period in which there was little fear in the markets, as the VIX stayed down at roughly 15%.

The parameter estimates for October 2008 are shown in Table 5. Notice in these estimates that the

Day	Y_0	κ	Y	$\gamma^2/(2Y\kappa)$	$f(1)$	$f(3)$	Q_{31}	Q_{32}	Q_{33}	$\lambda(1)$	$\lambda(2)$	$\lambda(3)$	rel-err.
8th	0.0100	2.56	0.0604	0.7338	0.5	3.1	0.7	-1.4	0.7	-0.001	-0.000	0.020	0.0024
9th	0.0100	3.02	0.0577	0.8679	0.5	3.6	3.2	-6.3	3.1	-0.000	0.000	0.020	0.0131
10th	0.0100	2.34	0.0571	0.8343	0.5	4.0	1.1	-2.2	1.1	-0.001	-0.000	0.020	0.0026
13th	0.0100	4.33	0.0716	0.7851	0.5	3.2	0.4	-0.8	0.4	-0.001	-0.000	0.020	0.1137
14th	0.0100	4.51	0.0581	0.4600	0.5	3.2	0.2	-0.4	0.2	-0.001	0.000	0.020	0.0113
15th	0.0100	3.81	0.0696	0.6603	0.5	3.6	0.2	-0.5	0.2	-0.001	0.000	0.020	0.0022
16th	0.0100	2.73	0.0942	0.6843	0.5	4.0	0.5	-1.0	0.5	-0.001	0.000	0.020	0.0070

Table 5: *Parameter estimates for 2008 Crisis data. Calibration to VIX Options of October 2008, $\theta_0 = 3$, $\delta = .01$, $f(2) = 1$.*

regime is in the high state ($\theta_0 = 3$) and the risk-neutral probability of switching out is very low ($Q_{33} \approx -1$ so that $\mathbb{P}(\text{regime change}) \approx 1 - e^{-1/365} \approx .003$). These parameters characterize the fear at that time, which was the belief that things were going to get a lot worse. Indeed, implied volatility of high-strike VIX calls was not increasing during October 2008 because the VIX future was extremely high; the flat implied volatility of high-strike VIX options during the crisis is seen in Figure 10.

The parameter estimates for February 2011 are shown in Table 6. In contrast to those in Table 5, the regime is $\theta_0 = 2$ because there is certainly not a high-volatility state, but the probability of jumping to the high state looms as $Q_{22} \approx -18$ (the risk-neutral probability of a jump is significantly higher than before as $\mathbb{P}(\text{regime change}) \approx 1 - e^{-18/365} \approx .05$). Historically, February 2011 was a relatively calm period for the VIX (and the SPX), but high-strike VIX options are somewhat of an insurance contract against outlier events, and so they trade at a premium for the same reason that low-strike SPX put options trade at a premium. The implied volatilities of these VIX options are shown in Figure 11, where we see an increase in implied volatility for high strikes caused by the probability of jumping to the high-volatility regime, aka by crash-o-phobia.

Finally, we should make a few remarks on the sensitivity of the parameter estimation procedure. It was mentioned in Section 5.1.1 that calibration of the model in (2) is a non-convex optimization, and it is well-known that non-convex problems are sensitive to the initial guess that is input to the optimization

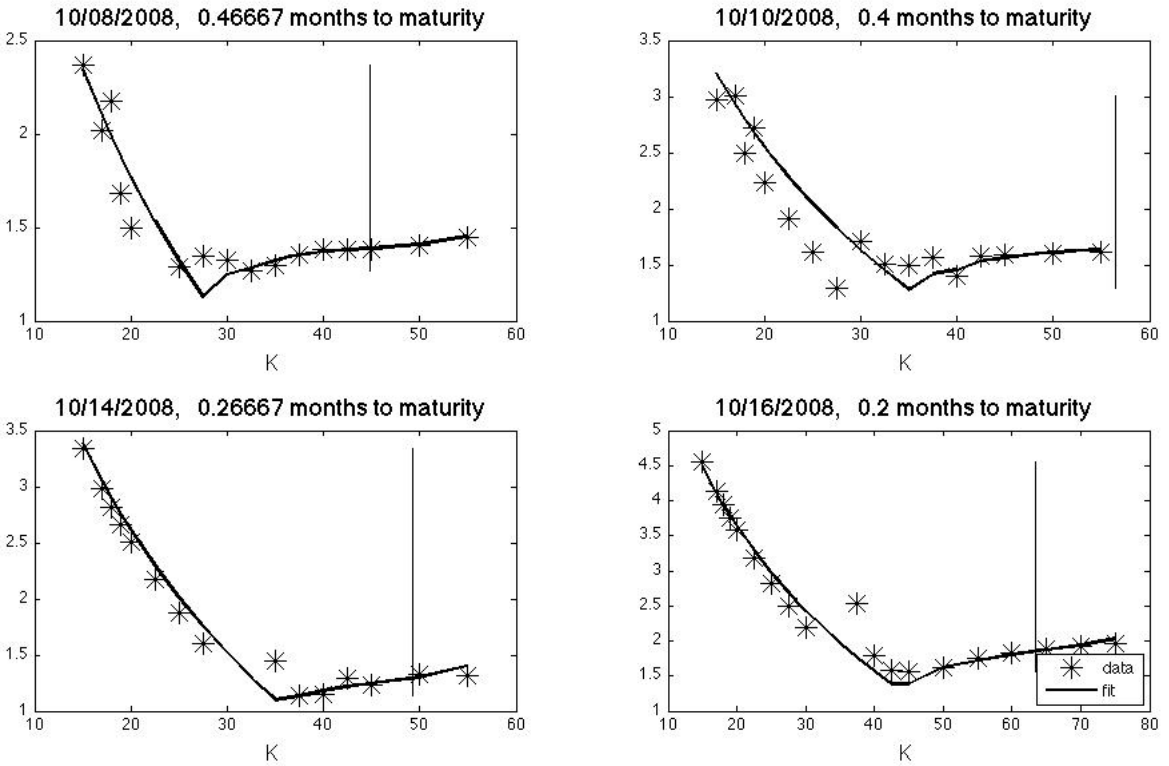


Figure 10: **Top:** Implied volatilities of VIX options during the Crisis of October 2008, fitted with the parameters of Table 5. The vertical is the VIX futures price; the belief during the crisis was that things were going to get a lot worse, so the VIX future was very high, and high-strike VIX options had low implied volatility.

algorithm. Hence, we see in Tables 5 and 6 that parameters associated with states that have little probability of occurring will not change much from their initial guess, as these parameters have little bearing on the fit (that is why we only fit Q_{θ_01} , Q_{θ_02} , and Q_{θ_03}).

6 Conclusion

Motivated by the frequent observation that the Heston stochastic volatility model cannot fit the implied volatilities of VIX options, we analyzed and implemented an extension which incorporates regime switching and jumps. Using asymptotic expansions of the Fourier transforms, we can efficiently price SPX and VIX options. When applied to market data, the model captures the implied volatility skews of both the SPX and VIX separately, but highlights a distinct discrepancy between the two markets. We also calibrated the model to VIX options from the 2008 financial crisis and to non-crisis data of 2011, and were able to relate the parameter estimates to the historical beliefs about volatility fears during these periods, confirming the importance of regime switches.

Day	Y_0	κ	Y	$\gamma^2/(2Y\kappa)$	$f(1)$	$f(3)$	Q_{21}	Q_{22}	Q_{23}	$\lambda(1)$	$\lambda(2)$	$\lambda(3)$	rel-err.
4th	0.0150	3.98	0.0290	0.6577	0.5	3.9	1.0	-18.6	17.5	-0.001	0.000	0.168	0.5013
7th	0.0150	4.06	0.0232	0.6237	0.5	4.0	1.0	-18.0	17.0	-0.001	0.000	0.181	0.6159
8th	0.0150	4.06	0.0195	0.6201	0.5	4.0	1.0	-18.0	17.0	-0.001	0.000	0.184	0.6003
9th	0.0150	4.19	0.0209	0.5459	0.5	3.8	1.0	-17.9	16.9	-0.001	0.000	0.192	0.5270
10th	0.0150	4.09	0.0344	0.6153	0.5	4.0	1.0	-18.0	17.0	-0.001	0.000	0.150	1.2601
11th	0.0150	4.07	0.0332	0.6217	0.5	4.0	1.0	-18.0	17.0	-0.001	0.000	0.128	1.3604
14th	0.0150	4.17	0.0127	0.8813	0.5	3.9	1.0	-18.0	16.9	-0.001	0.000	-0.148	0.5255
15th	0.0150	4.23	0.0135	0.7905	0.5	3.9	1.0	-18.0	17.0	-0.002	0.000	0.187	0.8480

Table 6: *Parameter Estimates for the Post-Crisis Data. Calibration to VIX Options of February 2011, $\theta_0 = 2$, $\delta = .01$, $f(2) = 1$.*

Acknowledgements

The authors thank Lissa Goldberg for discussion on regime models, as well as Jim Gatheral and two anonymous referees for their helpful comments.

References

- [1] Y. Ait-Sahalia, M. Karaman, and L. Mancini. The term structure of variance swaps, risk premia and the expectation hypothesis. Working paper, Princeton University, 2012. Available at <http://ssrn.com/abstract=2136820>.
- [2] G. Bakshi, C. Cao, and Z. Chen. Empirical performance of alternative option pricing models. *The Journal of Finance*, 52(5):2003–2049, 1997.
- [3] J. Baldeaux and A. Badran. Consistent modeling of VIX and equity derivatives using a 3/2 plus jumps model. Research Paper Series 306, Quantitative Finance Research Centre, University of Technology, Sydney, March 2012. Available at <http://ideas.repec.org/p/uts/rpaper/306.html>.
- [4] C. Bayer, J. Gatheral, and M. Karlsmark. Fast Ninomiya-Victoir calibration of the double-mean-reverting model. 2013. Available at http://papers.ssrn.com/sol3/papers.cfm?abstract_id=2210420.
- [5] T. Bollerslev and V. Todorov. Tails, fears, and risk premia. *Journal of Finance*, 66(6):2165–2211, December 2011.
- [6] P. Carr and R. Lee. Volatility derivatives. *Annual Review of Financial Economics*, 1:319–339, 2009.
- [7] P. Carr and D. Madan. Towards a theory of volatility trading. In M. Musiella, E. Jouini, and J. Cvitanic, editors, *Option Pricing, Interest Rates, and Risk Management*, pages 417–427. University Press, 1998.
- [8] P. Carr, D. Madan, and R. Smith. Option valuation using the fast Fourier transform. *Journal of Computational Finance*, 2:61–73, 1999.
- [9] P. Carr and L. Wu. Variance risk premiums. *The Review of Financial Studies*, 22:1311–1341, March 2009.
- [10] L. Chan, R.J. Elliott, and T.K. Siu. Pricing volatility swaps under heston’s stochastic volatility model with regime change. *Applied Mathematical Finance*, 14(1):41–62, 2007.
- [11] L. Chan, R. J. Elliott, J.W. Lau, and T.K. Siu. Pricing options under a generalized Markov-modulated jump-diffusion model. *Stochastic Analysis and Applications*, 25(4):821–843, 2007.
- [12] S. Chung, W. Tsai, Y. Wang, and P. Weng. The information content of the S&P 500 index and VIX options on the dynamics of the S&P 500 index. *Journal of Futures Markets*, 31(12):1170–1201, 2011.
- [13] R. Cont and T. Kokholm. A consistent pricing model for index options and volatility derivatives. *Mathematical Finance*, 23(2):248–274, 2013.

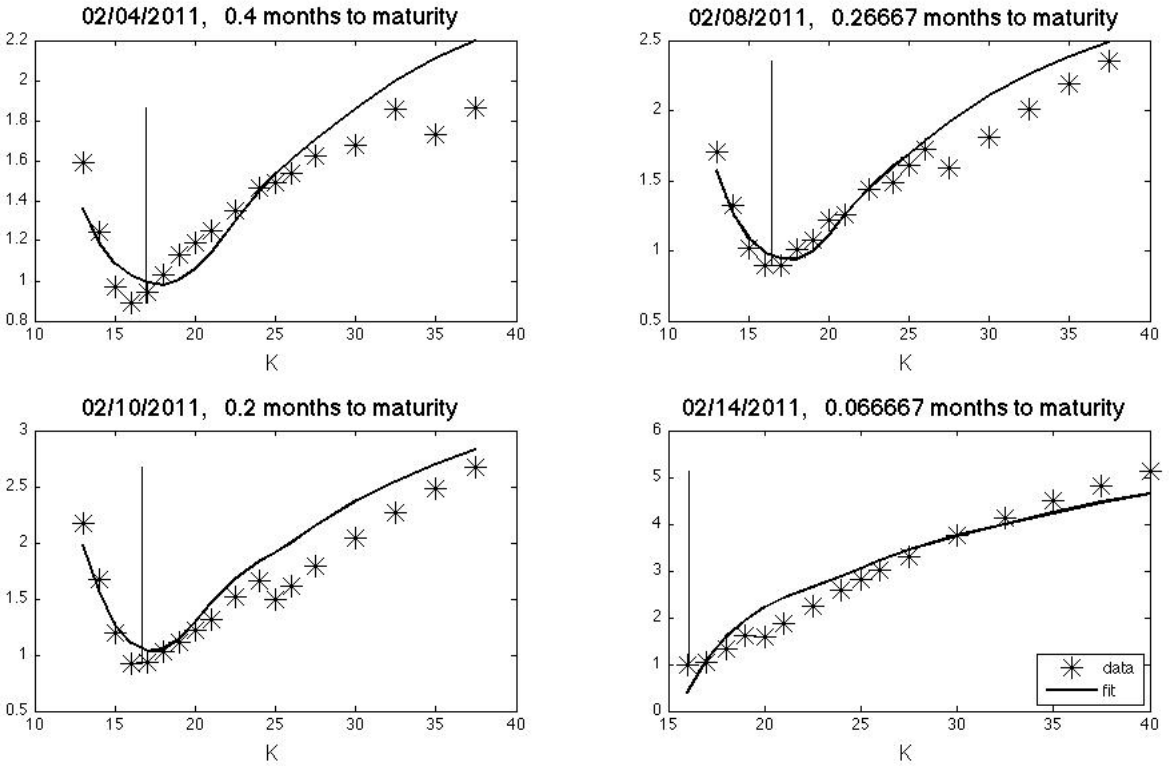


Figure 11: **Top:** Implied volatilities of VIX options during February 2011, fitted with the parameters of Table 6.

- [14] R. Daigler and Z. Wang. The performance of VIX option pricing models: Empirical evidence beyond simulation. *The Journal of Futures Markets*, 31(3):251281, 2011.
- [15] G. Drimus. Options on realized variance by transform methods: a non-affine stochastic volatility model. *Quantitative Finance*, 2012. forthcoming.
- [16] J. Duan and C. Yeh. Jump and volatility risk premiums implied by VIX. *Journal of Economic Dynamics and Control*, 34(11):2232–2244, November 2010.
- [17] D. Duffie, D. Filipovic, and W. Schachermayer. Affine processes and applications in finance. *Annals of Applied Probability*, 13:984–1053, 2003.
- [18] D. Duffie, J. Pan, and K. Singleton. Transform analysis and asset pricing for affine jump-diffusions. *Econometrica*, 68:1343–1376, 2000.
- [19] B. Eraker. Do stock prices and volatility jump? Reconciling evidence from spot and options prices. *The Journal of Finance*, 59(3):1367–1404, 2004.
- [20] J.P. Fouque and M. Lorig. A fast mean-reverting correction to Heston’s stochastic volatility model. *SIAM Journal on Financial Mathematics*, 2:221–254, 2011.
- [21] J.P. Fouque, G. Papanicolaou, R. Sircar, and K. Sølna. *Multiscale Stochastic Volatility for Equity, Interest Rate, and Credit Derivatives*. Cambridge University Press, 2011.
- [22] J. Gatheral. *The Volatility Surface: A Practitioner’s Guide*. Wiley, 2006.

- [23] J. Gatheral. Consistent modeling of SPX and VIX options. Presented at The Fifth World Congress of the Bachelier Finance Society in London, 2008. Available at: http://www.math.nyu.edu/fellows_fin_math/gatheral/Bachelier2008.pdf.
- [24] J. Hamilton. Regime switching models. In S. Durlauf and L. Blume, editors, *The New Palgrave Dictionary of Economics*. Palgrave Macmillan, 2nd edition, 2008.
- [25] S. Heston. A closed-form solution for options with stochastic volatility with applications to bond and currency options. *Review of Financial Studies*, 6:327–343, 1993.
- [26] E. Hillebrand. Neglecting parameter changes in GARCH models. *Journal of Econometrics*, 129(1-2):121–138, 2005.
- [27] S. Howison, A. Rafailidis, and H. Rasmussen. On the pricing and hedging of volatility derivatives. *Applied Mathematical Finance*, 11(4):317–346, 2004.
- [28] A. L. Lewis. *Option Valuation under Stochastic Volatility with Mathematica Code*. Finance Press, 2000.
- [29] V. Linetsky. Spectral methods in derivative pricing. In *Handbooks in Operations Research and Management Science: Financial Engineering*, volume 15, chapter 6, pages 223–299. Elsevier B.V., 2007.
- [30] D. Madan and M. Yor. The S&P 500 index as a Sato process travelling at the speed of the VIX. *Applied Mathematical Finance*, 18(3):227–244, 2011.
- [31] J. Mencía and E. Sentana. Valuation of VIX derivatives. Working Papers wp2009_0913, CEMFI, December 2009. Available at: http://ideas.repec.org/p/cmf/wpaper/wp2009_0913.html.
- [32] A. Sepp. Pricing options on realized variance in the Heston model with jumps in returns and volatility. *Journal of Computational Finance*, 11(4):33–70, 2008.
- [33] Z. Song and D. Xiu. A tale of two option markets: State-price densities implied from S&P 500 and VIX option prices. Working paper, Chicago Booth, 2012. Available at http://papers.ssrn.com/sol3/papers.cfm?abstract_id=2013381.
- [34] G. Tauchen and V. Todorov. Volatility jumps. *Journal of Business and Economic Statistics*, 29:356–371, 2011.